REGULAR ARTICLE

blood advances

Structure of shear-induced platelet aggregated clot formed in an in vitro arterial thrombosis model

Dongjune A. Kim and David N. Ku

George W. Woodruff School of Mechanical Engineering, Georgia Institute of Technology, Atlanta, GA

Key Points

- A shear-induced platelet aggregated clot is made of VWF surrounding billions of platelets to occlude a 2.5-mm lumen.
- Platelet aggregates grow as long, thin strings reaching across the lumen, then coalesce sideways, creating an unusual structure.

The structure of occlusive arterial thrombi is described herein. Macroscopic thrombi were made from whole blood in a collagen-coated, large-scale stenosis model with high shear flow similar to an atherosclerotic artery. The millimeter-sized thrombi were harvested for histology and scanning electron microscopy. Histological images showed 3 distinctive structures of the thrombus. (1) The upstream region showed string-like platelet aggregates growing out from the wall that protrude into the central lumen, with red blood cells trapped between the strings. The strings were >10 times as long as they were wide and reached out to join the strings from the opposite wall. (2) Near the apex, the platelet strings coalesced into a dense mass with microchannels that effectively occluded the lumen. (3) In the expansion region, the thrombus ended abruptly with an annulus of free blood in the flow-separation zone. Scanning electron microscopy showed dense clusters of spherical platelets upstream and downstream, with amorphous platelets in the occluded throat consistent with prior activation. The total clot is estimated to contain 1.23 billion platelets with pores 10 to 100 μm in diameter. The results revealed a complex structure of arterial thrombi that grow from their tips under high shear stress to bridge the 2.5-mm lumen quickly with von Willebrand factor platelet strings. The occlusion leaves many microchannels that allow for some flow through the bulk of the thrombus. This architecture can create occlusion or hemostasis rapidly with minimal material, yet can remain porous for potential delivery of lytic agents to the core of the thrombus.

Introduction

Arterial thrombosis in a stenosed coronary artery or carotid artery can lead to a myocardial infarction or an ischemic stroke. The formation of an occlusive thrombus in these arteries blocks blood flow, resulting in the patient's death. To stop blood flow, a thrombus must form under high shear rate (up to 400 000 s^{-1})[1] and be able to resist arterial blood pressure of >175 mm Hg.[2]

A thrombus can be distinguished by its mechanism of formation. A coagulation clot follows the classic Virchow's triad, which consists of stagnant blood flow, endothelial disruption, and hypercoagulability.[3] The primary structural component of a coagulation clot is fibrin, which is the final product of the coagulation cascade that entraps large amounts of red blood cells (RBCs). A coagulation clot is often referred to as a "red clot," because it appears to be red due to the presence of a large number of RBCs.[4,5] However, a coagulation clot can appear to be white if the clot is formed from artificially generated platelet-rich plasma lacking in RBCs but having an abundance of fibrin. Meanwhile, Casa et al[6] proposed an

Submitted 27 September 2021; accepted 20 January 2022; prepublished online on *Blood Advances* First Edition 27 January 2022; final version published online 6 May 2022. DOI 10.1182/bloodadvances.2021006248.

Requests for data sharing may be submitted to David N. Ku (david.ku@me.gatech.edu).

The full-text version of this article contains a data supplement.

© 2022 by The American Society of Hematology. Licensed under Creative Commons Attribution-NonCommercial-NoDerivatives 4.0 International (CC BY-NC-ND 4.0), permitting only noncommercial, nonderivative use with attribution. All other rights reserved.

alternative triad for shear-induced platelet aggregation (SIPA) clot formation: (1) a pathologically high shear rate, (2) a collagen surface for von Willebrand factor (VWF) attachment, and (3) platelets and VWF in sufficient concentrations. Thus, a SIPA clot is composed predominantly of platelets and VWFs, with a few RBCs, a finding further supported by Ku and Flannery,[7] who found that 80% of a SIPA clot consists of platelets. SIPA clots are commonly called "white clots" because of the lack of RBCs. A coagulation clot is implicated in deep venous thrombosis, whereas a SIPA clot is more strongly implicated in arterial thrombosis.[5,8] The structure of these blood clots provides clues as to how they form and how we can best treat patients who have a heart attack or stroke.

The structure of these blood clots has recently become a hot topic, in conjunction with the emergence of thrombectomy.[9-12] Previous approaches using in vivo animal models with intravital fluorescence imaging[13] have a spatial resolution limit that impedes the investigation of the microstructures of blood clots.[5] In contrast, thrombi extracted during a thrombectomy can subsequently be imaged via scanning electron microscopy (SEM)[14-16] or microscopy of histologic sections.[10,17] However, this thrombectomy-based approach has weaknesses. First, extracted thrombi can be deformed or destroyed during a process of thrombectomy. Second, there is an inevitable time delay between thrombi formation and structural investigation. When a SIPA clot forms in a stenotic artery and blood flow ceases, a coagulation clot may form around the SIPA clot because of the stagnant blood. We hypothesized that occlusion in a stenotic artery is caused by a SIPA clot that has a distinctive structure and composition compared with the coagulation clot. The structure is not homogeneous, but shows anisotropy from the high shear growth.

In this study, we developed an in vitro flow system that can generate a macroscopic thrombus under arterial hemodynamic conditions that would enable us to retrieve an intact SIPA specimen for the structural investigation. To study the structure of the SIPA clot, we analyzed multiple SEM and histology images. The characteristic structure of the arterial thrombus presented in this study may give insight into the mechanism of occlusion, along with possibilities of preventing or treating arterial thrombosis.

Materials and methods

High-shear glass tube model

To generate a SIPA clot, lightly heparinized (3.5 IU/mL) porcine whole blood (400 mL) was perfused through an in vitro flow system. A high flow rate (~1 L/min) was necessary to generate a high shear rate (>3500 s^{-1}) in a glass tube with a stenosis diameter of 2.5 mm. To accommodate this requirement, a closed flow loop was developed with 2 reservoirs for a constant pressure head of 30 mm Hg (Figure 1A). Before the blood perfusion, the stenotic region of the tube was coated with 100 μg/mL type 1 fibrillar collagen solution (Chronopar; Chrono-log Inc.) in 0.9% saline by pipetting 60 μL at the stenosis and incubating it in a container at room temperature for 24 hours to generate an adhesive surface. An hour after the moment when a collagen solution was added to the tube, the tube was rotated 180°, once.

Coagulation clot generation

Porcine blood was treated with 3.2% sodium citrate (10% in volume) during transportation and then recalcified with $CaCl_2$ to a final concentration of 10 mM.[18,19] The recalcified porcine blood was left at rest for at least 30 minutes at room temperature to form a stable red coagulation clot.

SIPA clot generation in a closed flow loop

Heparinized (3.5 IU/mL) porcine whole blood (~400 mL) was used to fill the flow loop and perfused (Figure 1A) to generate a large SIPA clot. The glass tube (Figure 1B) had an inner diameter of 12 mm and an 80% stenosis. The Reynolds number (Re) was 334, and the white clot grew from the wall into the lumen, similar to the growth in the capillary tube experiment[20] where the Re was 162. The white SIPA clot grew in the stenotic region over time (supplemental Movie 1), and the roller pump was manually adjusted to reduce the flow rate and maintain a constant 30 mmHg pressure head (Figure 1C). The maximum shear rate reached over 10 000 s^{-1} with the initial flow rate (Figure 1D), which is in the range where rapid platelet accumulation (RPA) can occur.[21] When the roller pump flow rate reached a minimum level (50 mL/min), the pump was turned off, but maintained the pressure head without significant change. We defined the occlusion time as when the pump was turned off. The low flow rate was less than 50 mL/min, and the SIPA clot was left to mature. Thus, the circuit was left for an additional 30 minutes to achieve full occlusion. The occlusion was found after the blood was drained from the circuit (Figure 1E-F; supplemental Movie 2), and the generated clot was retrieved from the tube gently. A total of 8 SIPA clots were generated in this study, and the consistency in gross appearance of all the specimens was remarkable. Two specimens were used for SEM imaging. Three clots were sectioned longitudinally and stained with Carstairs and VWF. Two clots were sectioned transversely and stained with Carstairs and VWF.

Computational fluid dynamics analysis

Computational fluid dynamics was used to quantify the shear rate distribution within the stenotic test section. The steady-flow simulation was performed with Ansys 19.1 (Ansys Inc., Pittsburgh, PA). Whole-blood flow was assumed to be a Newtonian fluid of 3.5 cP, and the flow was presumed to be laminar, incompressible, a steady continuum, and isothermal based on the Re of 334 of the experiments. A flow rate of 660 mL/min was applied at the inlet with a pressure of 0 at the outlet. Mesh convergence was achieved at 0.6 million hexagonal cells.

Arterial thrombosis model

SIPA clot growth in the glass tube was predicted in a quantitative, empirical high-shear thrombosis model.[21] The model is composed of a lag phase and an RPA phase defined by $t_{Lag} = 1.69 \times 10^6 S^{-1.2}$, where t_{Lag} is lag time and S is the wall shear rate. Thrombus growth rate during the RPA phase is expressed by time (t) and shear rate (S).

$$J = \begin{cases} 0, & t \leq t_{Lag} \\ ae^{bS} + ce^{dS}, & t > t_{Lag} \end{cases}$$

Constants a, b, c, and d are given in Table 1. The lower and upper confidence limit of thrombus growth are denoted by J_{MIN} and J_{MAX}, respectively.

The assumptions of Poiseuille flow were applied at the throat, and the shear rate was defined by

$$S_{Cir} = \frac{32Q}{\pi d^3},$$

where Q is the flow rate and d denotes the channel diameter. An initial flow rate of 0.66 mL/min and a diameter of 2.5 mm at the throat was

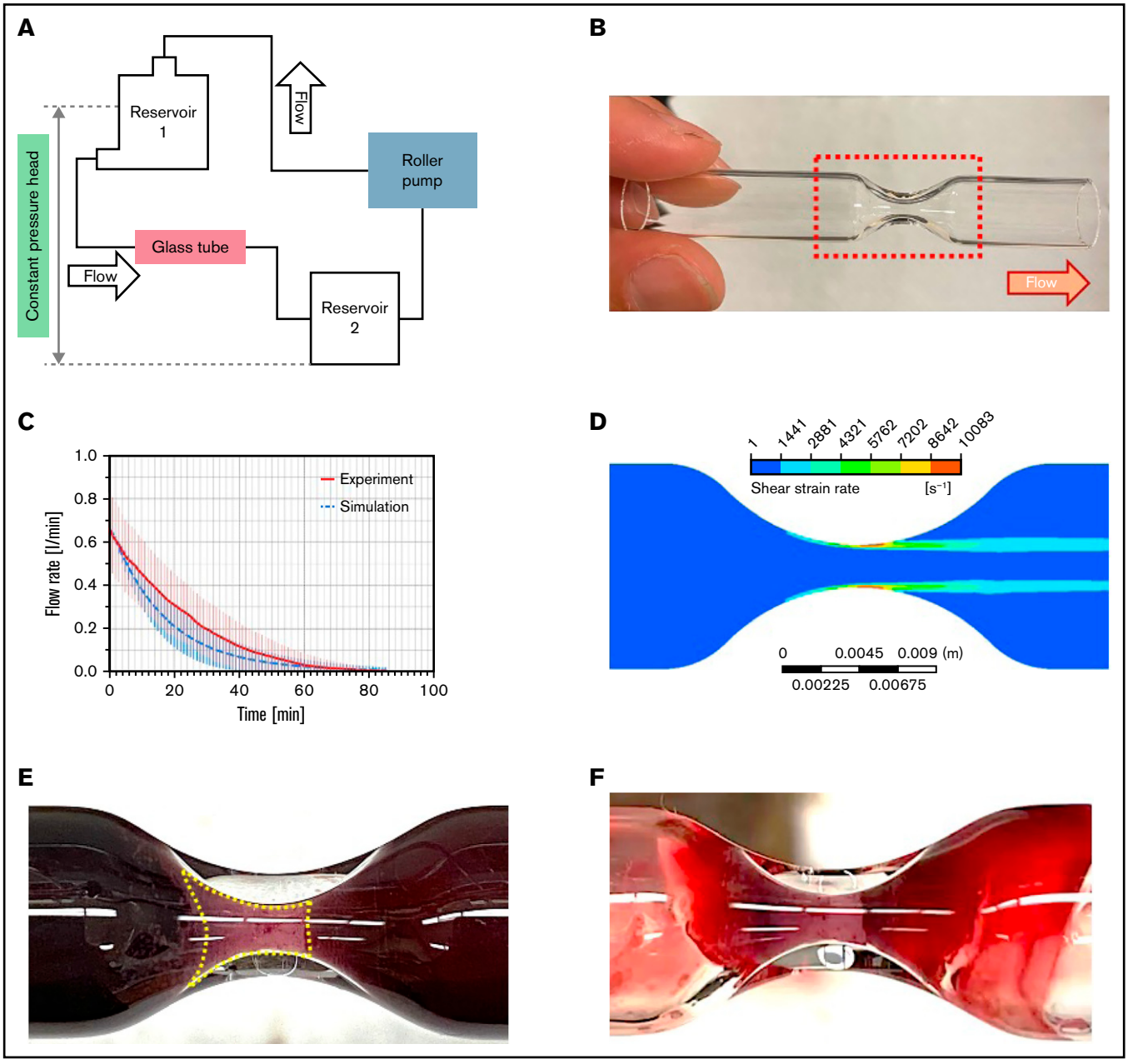

Figure 1. In vitro flow loop for generating a SIPA clot. (A) A constant-pressure closed loop circuit with a roller pump was developed to generate a clot in (B) a collagen-coated glass stenosis that has a throat diameter of ~2.5 mm. A total volume of 400 mL of blood was circulated through the flow loop. (C) To maintain a constant 30-mm Hg pressure head, the roller pump flow rate was reduced as the clot grew over time (red, mean of 8 with standard deviation, shown by vertical lines) as compared with the simulated flow rate in an empirical model of SIPA thrombus growth rate (blue, upper and lower limit displayed in the bars). (D) The initial maximum shear rate in the throat was greater than 10 000 s^{-1}. The area of high shear is consistent with the thrombus location in the stenosis. (E) The SIPA clot occluded the stenosis with a trumpet-like shape. The boundary of the SIPA clot is highlighted by the yellow dotted line. (F) The glass tube with the SIPA clot after blood was drained, showing the extension of the thrombus at the wall both upstream and downstream of the throat.

Table 1. Constants for RPA-phase thrombus growth rate equation in the empirical model

	a	*b* (×10^{-4})	*c*	*d* (×10^{-6})
J_{MIN}	−28.3	−1.00	27.4	−10.0
J_{AVG}	−31.3	−1.45	30.7	−6.81
J_{MAX}	38.2	−1.81	36.6	−5.92

used, and the channel diameter was updated every second as thrombus growth increased in the tube.

SEM imaging

SEM illustrates the morphology and density of the platelets. Blood clots were fixed in a 10% formalin solution for more than 24 hours. A fixed blood clot was submerged in successive ethanol

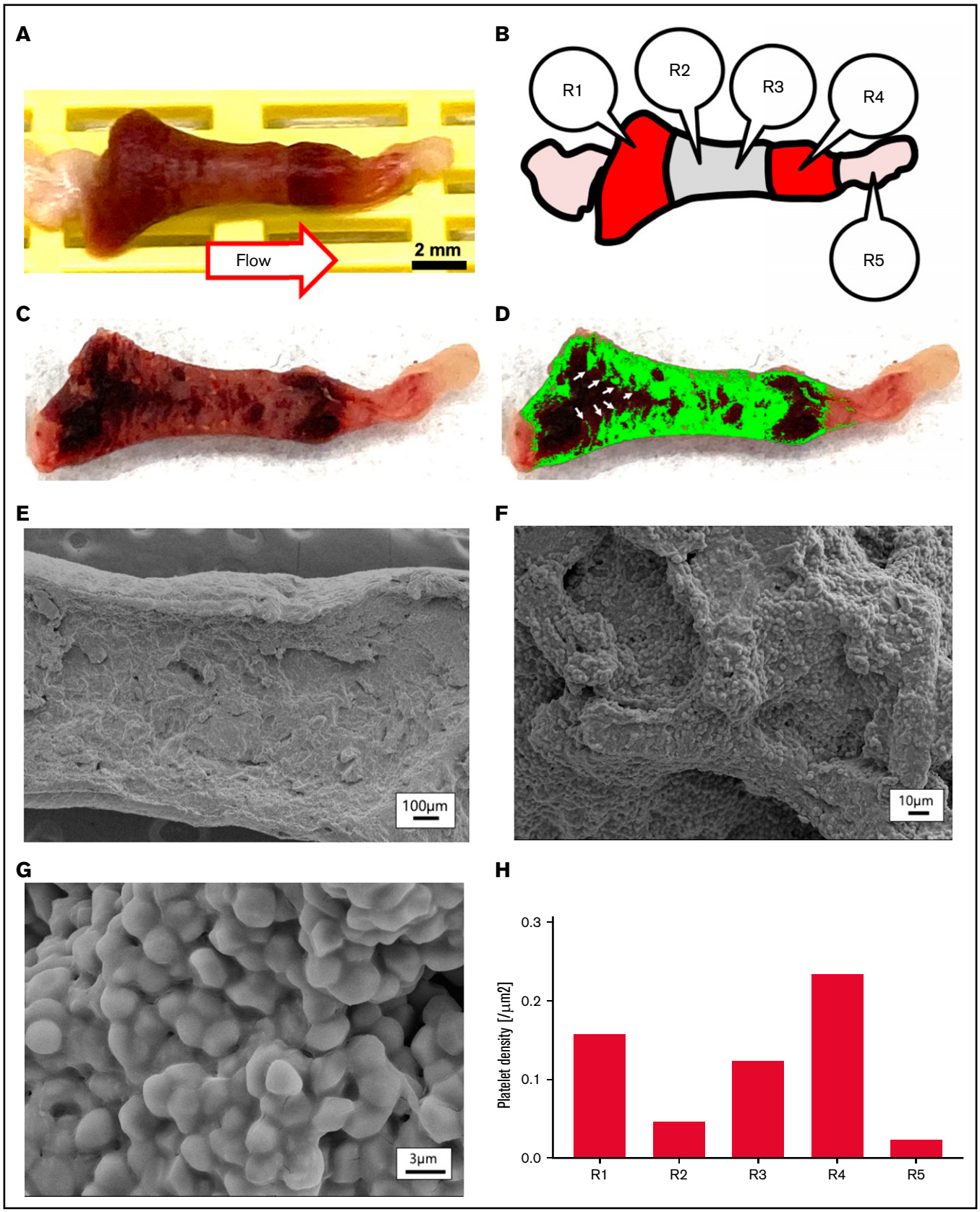

Figure 2. Harvested SIPA clot and SEM images. (A) A SIPA clot retrieved from the large glass tube was formalin fixed and dehydrated with ethanol. (B) Schematic of a SIPA clot with regions of interest (R1-R5). (C) A SIPA clot cut in half to expose the cross section. (D) The platelet-rich white region is highlighted in green, showing fingers of platelet aggregates (white arrows). (E-G) SEM image of SIPA clot region of interest R4. (E) Low magnification SEM image of the SIPA clot showing the dense core of the thrombus. (F) Moderate magnification SEM image of the SIPA clot illustrating a textural surface of platelet aggregates. (G) High-magnification SEM image of the SIPA clot showing amorphous platelets that are likely activated with degranulation. (H) Platelet density from SEM images of regions R1 to R5.

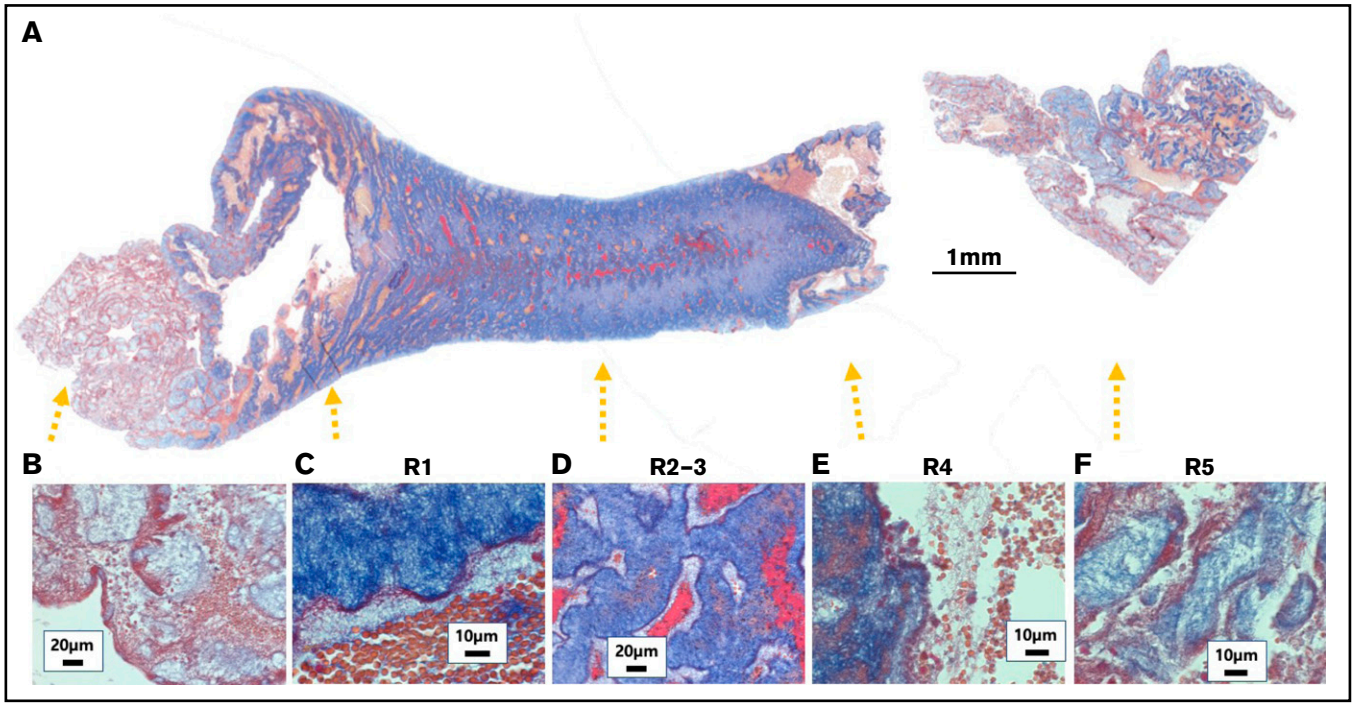

Figure 3. Carstairs staining of a SIPA clot in the longitudinal direction. (A) The trumpet-like morphology of the gross clot was preserved. (B-F) Each end of the clot showed small platelet aggregates with fibrin. (C) Upstream of the throat, the thrombus had platelet aggregates protruding toward the lumen with string or fingerlike shapes alternating with trapped RBCs. Some strings were 10 times longer than they were wide. (D) The apex of stenosis was fully occluded with platelets. Some fibrin was found in the center of the lumen and pores. (E) Downstream, the clot was present at the center and near the wall; whereas the annulus between the 2 had sparce RBCs and fibrin without platelet aggregates. R1 to R5 correspond with the regions of interest shown in the schematic in Figure 2B.

concentrations of 25%, 50%, 75%, 80%, and 90% for 15 minutes each and rinsed with distilled water. After overnight air drying, the samples were sputter coated with Au and imaged by SEM (SU8230; Hitachi).[22]

Histology and immunohistochemistry

The histology revealed the composition and structure of the thrombus. The blood clots were fixed in formalin and embedded in paraffin for further histological and immunohistochemical analyses. The paraffin block holding the clot was cut into 5-μm-thick slices and deparaffinized. Carstairs's staining method[23] was used to stain the platelets light blue, the fibrins red, the RBCs yellow, and the white blood cells (WBCs) black. Separately, VWF immunohistochemistry was conducted with the Polink-2 plus a DAB (3,3′-diaminobenzidine) detection system (GBI Labs, Mukilteo, WA) and an anti-VWF antibody (primary antibody; Biocare Medical, Pacheco, CA).[24] We added ≥100 μL of primary antibody, incubated the sections in a moist chamber overnight at room temperature, and later counterstained them with Mayer's hematoxylin.

Results

The thrombus developed over 1 hour to occlusion, and blood flow ceased in 60 ± 17 minutes (Figure 1C; n = 8). CFD was performed to quantify the shear rate at the stenosis (Figure 1D). The high-shear thrombosis model of Mehrabadi et al[21] was used to stimulate the flow rate, with the initial flow rate value from the experimental data (660 mL/min), to estimate the occlusion time to aid in the design of the experiment. The model estimated occlusion at ∼71 minutes (Figure 1C), confirming that our microfluidics system creates a thrombus similar to that created by our large-scale system. All occlusive SIPA clots had a similar trumpet-like shape with the horn opened against the flow (Figure 1F; supplemental Figure 1). After the flow circuit was drained, the SIPA clot was retrieved (Figure 2A) from the large glass tube for SEM imaging and histology.

Platelets are tightly packed in a SIPA clot at the throat of the stenosis

The retrieved gross clot was trumpet-shaped, similar to the one observed during the blood perfusion (Figures 1E-F and 2A; supplemental Figure 1) and had different colors in characteristic regions. At the upstream and the downstream portions, there were translucent yellow parts that were originally attached to the glass wall (Figure 2B; R5). These parts were thin sheets attached to the upstream region of the stenosis but became folded and tangled during detachment from the wall. We interpreted this yellow material to be the gross appearance of adherent VWF. The thrombus recovered from the throat of the stenosis was light red or pink (Figure 2B; R2 and R3). This stenotic region was predominantly a white clot. Far downstream of the throat was a region of dark red material that looked like a coagulated red clot (Figure 2B; R1 and R4). After formalin fixation and dehydration, we cut the clot in half in the flow direction to image the inner part of the clot (Figure 2C). The longitudinal section revealed string-like structures protruding toward the lumen (Figure 2C-D) that were up to 10 times longer than they were wide.

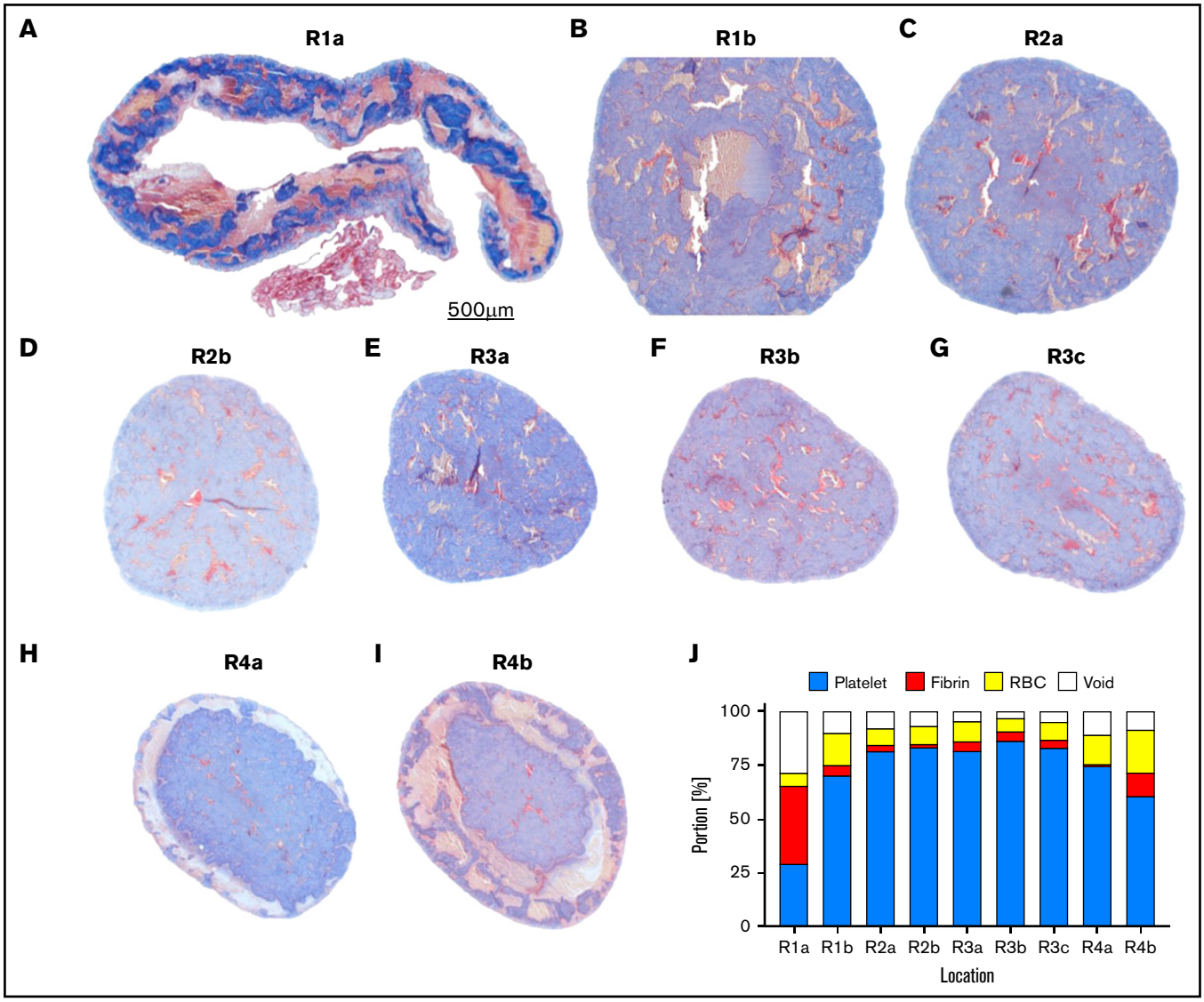

Figure 4. Carstairs staining of the SIPA clot in the transverse direction. (A-I) Starting from the upstream end, each section is spaced ~0.5 mm apart. (J) The plot shows portion of blood clot components (platelet, fibrin, RBC, and void) found in Figure 4 A to I. Sequential sections corresponding to the regions of interest indicated in Figure 2B (R1a-R4b).

The string- or finger-like structure was not preserved in the sectioned SEM images. Geological shapes were seen in the low-magnification images (Figure 2E) with layers of aggregates and some fibers. Meanwhile, the moderate magnification images displayed aggregates of numerous spheres that were ~2 μm in diameter, which were interpreted as individual, inactivated platelets (Figure 2F), whereas activated platelets should show spikelike filopodia and spreading disc morphology.[25] The platelet aggregates were easily seen in the high-magnification images (Figure 2G). To quantify how many platelets were packed in the clot, we manually counted recognizable spheres with a diameter greater than 1.5 μm in calibrated sections of the high-magnification SEM images. Using the observed 2-μm platelet thickness on the SEM images with an average value of 0.1 platelets per square micrometer (Figure 2H), we calculated a platelet density per volume of 0.05 platelets per cubic micrometer, and the total SIPA clot was estimated to contain 1.23 billion platelets.

The SIPA clot occlusion arises from strings of platelets and VWF coalescing with a porous structure

SIPA clots were stained using the Carstairs or VWF immunostaining method. Three clots were sectioned longitudinally, and the other 2 clots were sliced transversely. Consistent with the SEM results, Carstairs staining showed that the SIPA clot was dominantly occupied by platelets (Figures 3A and 4A-I; blue) and immunostaining indicated that VWF was present throughout the SIPA clot (Figure 5), proving that the SIPA clot is VWF and platelet-rich as opposed to coagulation clots (supplemental Figures 2 and 3; control). Meanwhile, although the coagulation cascade is unlikely because of pathological high shear conditions, Carstairs staining revealed a few RBCs (yellow to orange) and some fibrin (red) in the clot (Figure 3). Presumably, RBCs become trapped and fibrin forms in stagnant pockets within the overall platelet thrombus or after occlusion

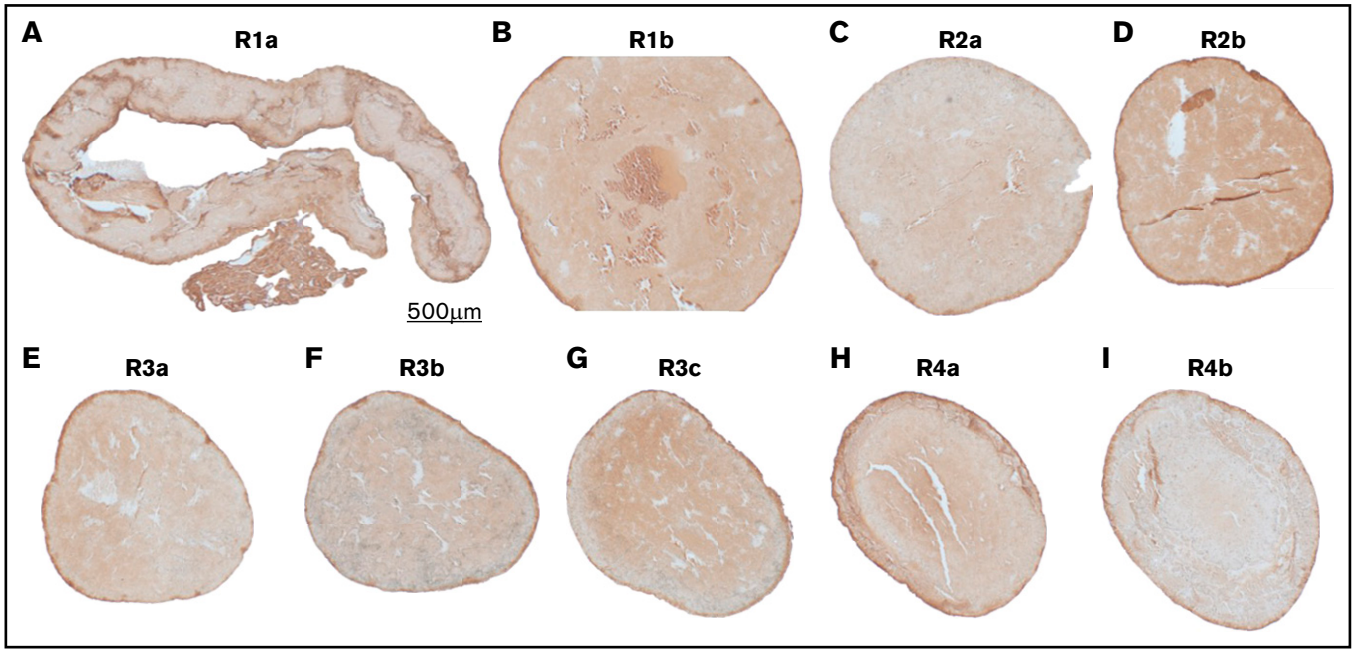

Figure 5. VWF immunostaining of the SIPA clot in the transverse direction. Starting from the upstream, each section is spaced ~0.5 mm apart. Sequential sections corresponding to the regions of interest indicated in Figure 2B (R1a-R4b).

formation. Thus, the void region and the space occupied by RBCs and fibrin are assumed to be pores or valleys that were formed during SIPA clot formation.

The histological appearance reflected the gross appearance seen macroscopically (Figure 2C). The transparent, thin sheets in the far upstream region was dominantly VWF with few platelets, but also contained some fibrin (Figure 3B). The small, dispersed platelet aggregates were surrounded by fibrin (Figure 3B). As the stenosis converged, the platelets and trapped RBCs formed a striped pattern (Figure 3A,C). The platelet fingers alternated with stripes of RBCs that were trapped in the space between the platelet aggregates (Figure 3C). In the throat of the stenosis where the shear rate and SIPA were expected to accelerate, axisymmetric structures were present that contained a few trapped RBCs. Fibrin was visible in pores near the center of the lumen (Figure 3A,D). A thin zone of light blue can be seen just next to the wall, representing fewer platelets attached to the wall. Then, a color gradation of dark blue to medium blue extended to the center of the lumen representing dense platelets at the periphery and less dense platelets at the center (Figure 3A). Downstream of the stenosis in the expansion region, the core protruded into the center, but the thrombus separated from the wall, consistent with a flow-separation zone (Figure 1D). The separation zone was filled with loose RBCs, but not a platelet mass (Figure 3E).

Another SIPA clot was sectioned transversely and stained using the Carstairs and VWF immunostaining method. The upstream section showed a large number of trapped RBCs and a small number of dispersed platelet aggregates with fibrin (Figure 4A) and VWF (Figure 5A). The next section showed a large hole at the center and trapped RBCs and some fibrin in the pores (Figure 4B). The stenotic sections revealed thrombus that completely occluded the lumen by a mass of blue platelets interspersed with pores filled with RBCs (Figure 4C-G). Further downstream past the stenosis, there was a bull's eye or target appearance, with a central dense core surrounded by a layer of loose RBCs and then a thin layer of platelets at the wall (Figure 4H-I). As it got close to the throat, the platelet proportion increased, but the fibrin proportion decreased (Figure 4J).

Summarizing the findings from histology and SEM, the occluded throat section was composed of 80% dense platelets and VWF with 5% fibrin and many channels ranging from 10 to 100 μm. The upstream region showed long VWF strands adherent to the wall without large platelet aggregates where shear rates were less than 1400 s^{-1} (Figure 2D; white arrows). Stripes of platelet aggregates and individual RBCs were found in upstream and downstream regions, where more inactivated platelets are seen on SEM than the stenosis region (Figure 2G from the downstream throat R4 in Figure 2B and supplemental Figure 4 from the throat R3 in Figure 2B). Platelets within the stenosis throat were mostly misshapen consistent with prior activation by the very high shear rate (up to 9000 s^{-1}; Figure 1D). The downstream end of the thrombus on SEM showed a protruding central core of round platelets that appeared not to have been activated. Surrounding the core was an annulus without thrombus, where there was flow separation with a lower shear rate. At the wall was a thin ring of VWF and small aggregates hugging the collagen surface and extending throughout the recirculation region.

The SIPA clot is rich in VWF, especially near the wall

Staining for VWF (brown) was found throughout the SIPA clot, but was not present in a platelet-rich plasma clot formed under stagnant conditions (supplemental Figure 3). In the longitudinal and transverse directions, the immunostaining results showed that VWFs

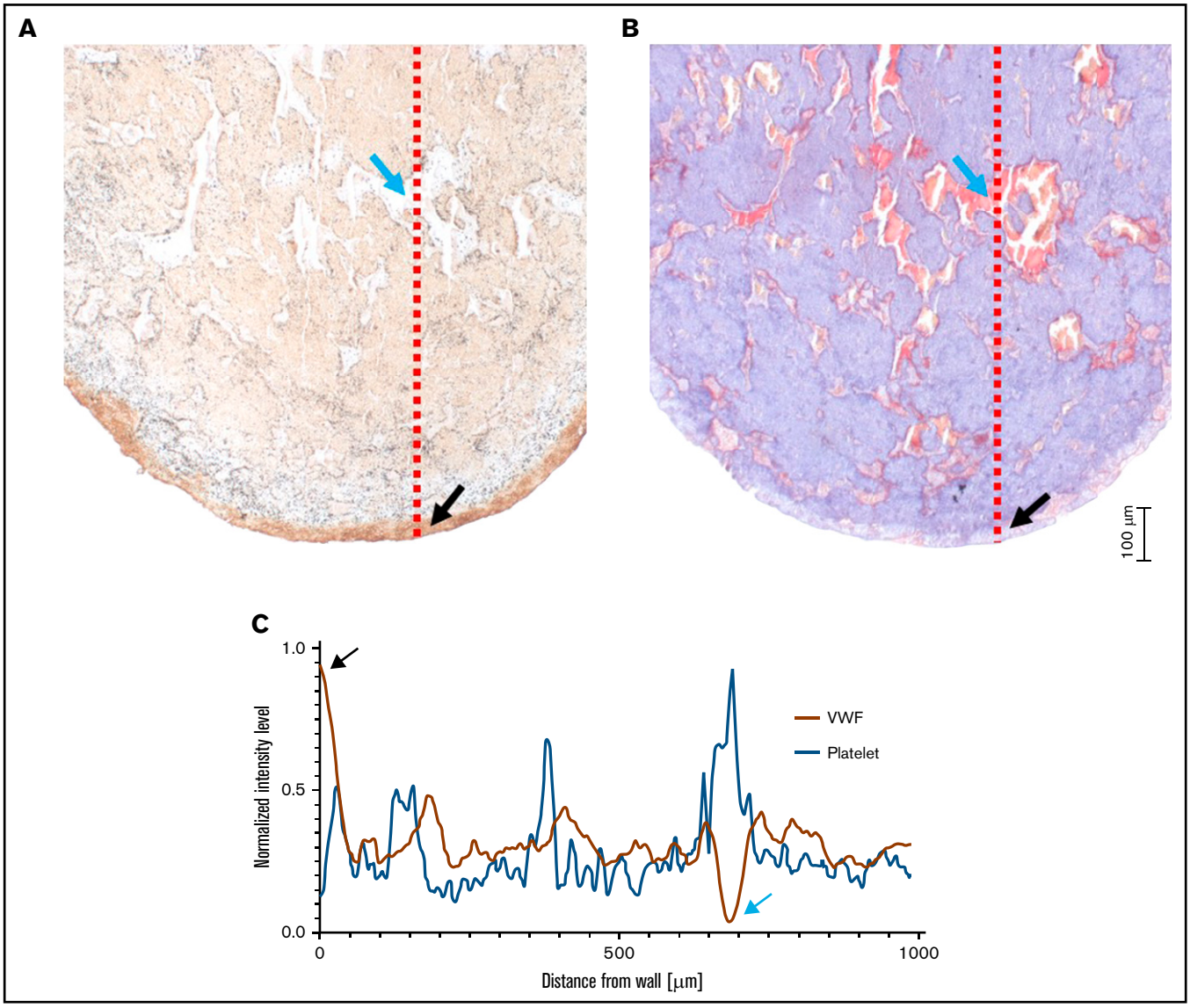

Figure 6. Comparison of VWF and platelet density near the channel wall. VWF staining (A) and Carstairs staining (B) of a SIPA clot in the transverse direction (original magnification, ×10). (C) Normalized intensity level along the red lines in panels A and B. Near the lumen wall, VWF was concentrated and dark, yielding low-intensity levels; whereas the Carstairs-stained platelet was light at the wall, corresponding to a high-intensity level. Black arrows indicate the starting point close to the wall, and blue arrows indicate a pore in the clot.

were concentrated at the edge where the clot adjoined the wall (Figure 5). In contrast, in the Carstairs staining result, the blue coloring was lighter near the wall, indicating that fewer platelets aggregated at the wall during the lag phase (Figure 4). This complementary density of VWF and platelet is quantified in Figure 6, which plots the normalized intensity level of VWF and platelets from wall to lumen. Therefore, when the SIPA clot started to develop, a large amount of VWFs must have accumulated at the wall first, to capture the marginated platelets. The thickness of this VWF-rich layer was ~20 μm, and it had fewer platelets.

Discussion

SIPA clots were generated in a closed in vitro flow loop to investigate SIPA clot structure. The size of the generated SIPA clot was anatomically relevant to diseased arteries (2~2.5 mm in diameter and 5 mm in length) and had a trumpet-like shape with the horn facing upstream. This SIPA clot was 2- to 20-fold larger in diameter than previously generated SIPA clots,[26,27] which enabled us to collect the clot with the structure intact. We sectioned the specimens longitudinally or transversely. SEM images showed that the platelets were tightly packed in the clot with a density of 0.1 platelets per square micrometer, indicating that the 1.23 billion platelets were aggregated in the SIPA clot, which is significantly different from previous images of RBC-rich blood clots.[14-16] Spherical platelets were found in the SEM images, and its morphology was similar to the platelets found in the ultra–densely packed region of the mouse puncture injury model used by Tomaiuolo et al.[28] The histological images showed consistent results in which the clot was VWF platelet rich, and RBCs were trapped in the pores, which is strikingly similar to

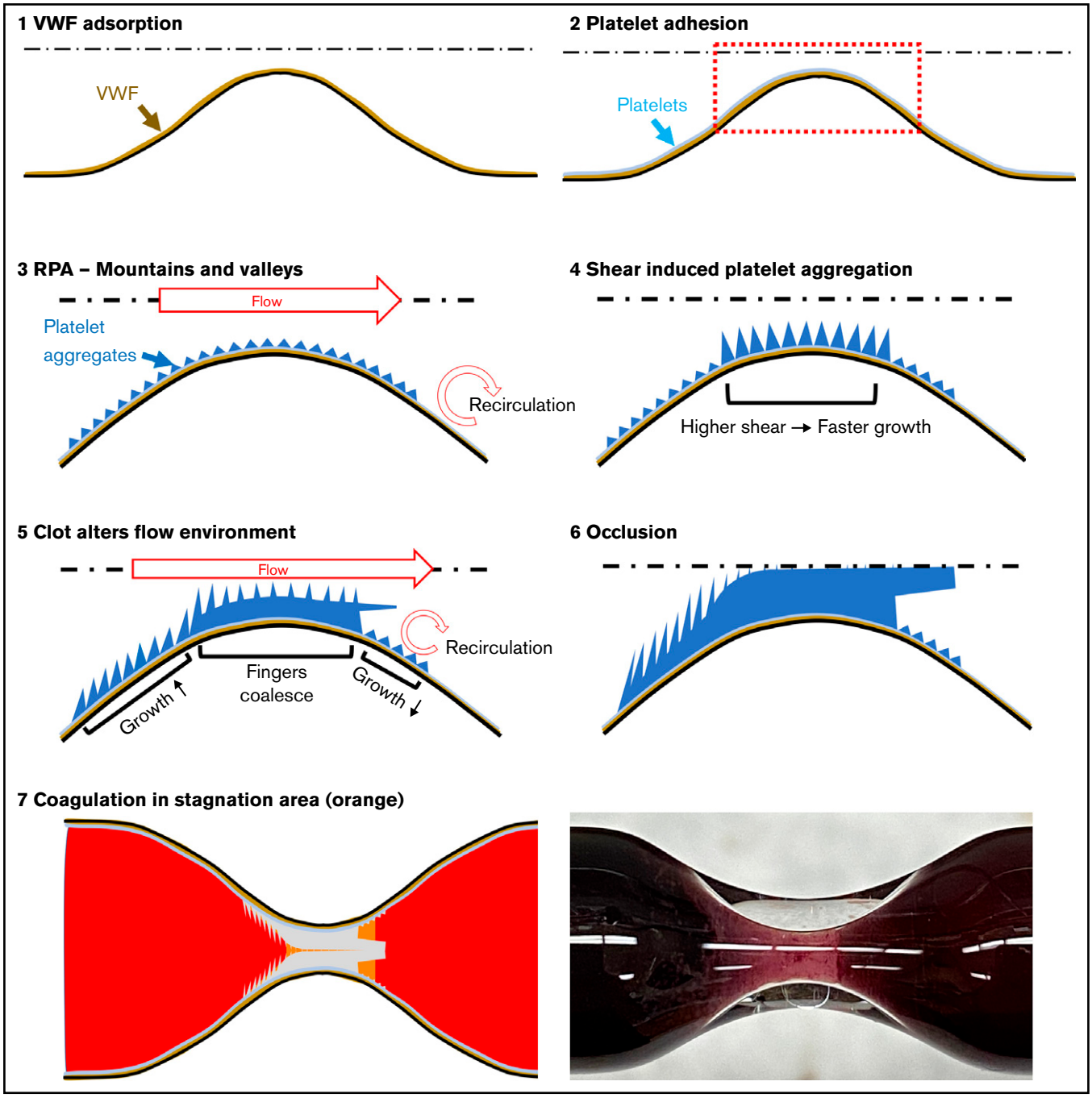

Figure 7. Process of SIPA clot formation in a large stenotic vessel. (1) Schematic showing the bottom half of a stenosed vessel. The dotted line indicates the axisymmetric centerline. VWF (brown) adsorption onto the collagen surface under high shear rate. (2) Sparce platelet adhesion (light blue) to the surface. (3) Details of the dotted box in panel 2. RPA begins and forms mountains and valleys of platelet aggregates. (4) SIPA accelerates the thrombus growth with higher shear rate near the apex. (5) Growing thrombus at the apex alters the flow environment and creates larger recirculation region downstream. (6) SIPA clot occludes the vessel. (7) Final SIPA clot (light gray) comparison between the schematic (left) and the experimental photograph (right).

SIPA clots formed in our mouse arterial thrombosis model.[29] The high platelet content of our SIPA clot in both SEM and histological images are also consistent with the composition of arterial clots found in clinical studies.[5,8] Our SIPA thrombi look very similar to the platelet-rich clinical clots in Staessens et al,[8] showing platelet content between 90% and 50%, as well as VWF staining. Our SIPA clots appear consistent with the platelet-rich regions in the clinical blood clot images described in Tutwiler et al,[30] Staessens et al,[10] and Chernysh et al.[16] Note that our fresh thrombi were not given time to contract into a mature clot. The clinical samples were retrieved without orientation and may represent a mixture of a central white clot mixed with coagulation clots upstream and downstream

formed by stagnant blood after occlusion. Our thrombi showed more spatial detail than harvested pieces of clinical thrombus. Nonetheless, our clots showed consistency with the retrieved clinical clots that were platelet rich.

The SIPA clot structure revealed herein may be explained by a 7-step process for SIPA clot formation.[31] The process starts with high wall shear rates (step 1) and VWF adsorption onto the collagen surface (Figure 7-1; step 2). In this study, the SIPA clot had a high VWF density on the wall, but sparse platelets compared with the lumen side (Figure 7-2). The plasma VWF must be important for the lag phase (step 1-2), as platelets need to be captured at the wall (step 3-4). Casa et al[32] found that plasma VWF is more important than platelets in forming occlusive SIPA clots. When a sufficient amount of insoluble VWF accumulates at the wall, some platelets are captured (step 3-4) and activated. These mural platelets can make new, highly reactive surfaces by releasing α-granules of VWF (step 5). VWF release from α-granules are necessary to initiate the RPA phase (step 5-7) and the subsequent vessel occlusion.[29] The histological images show that there was a marked transition from light blue to dark blue all the way to the lumen. This light blue layer was $\sim$20 μm thick, which is comparable to the thrombus thickness hypothesized by Bark et al[33] for the lag phase, as a transition from the lag phase to the RPA phase. Between the 20-μm wall layer and the center of the lumen, string-like structures protruding from the wall into the lumen were found in the longitudinally cut SIPA clot (Figure 2C) and the Carstairs-stained slice in a longitudinal direction (Figure 3A). This string structure has been noted by previous investigators for VWF+platelets and was prominent at the upstream section (Figure 2B; R1), with RBCs trapped between the fingers. Past studies also observed these SIPA clot structures, which was referred to as "fingers" in expanded polytetrafluoroethylene vascular graft tubing[26] and the glass capillary tube,[27] but this is the first report, to our knowledge, of a string-like structure in an intact, oriented, occlusive SIPA clot. Inhibiting α-granule release of VWF may interrupt the long VWF+platelet fingers, thus preventing vessel occlusion.[29]

These fingers grew from the wall toward the center of the lumen to occlude the large ($\sim$2.5 mm in diameter) channel (Figure 7-3). The fingers appear to have been growing faster near the apex related to a higher shear rate that promotes increased thrombus growth rate[21] (Figure 7-4). The faster growth at the apex region can constrict the lumen, creating a recirculation area similar to that which Kim et al[20] observed in their capillary tube model that arrests SIPA distally (Figure 2B; R4). Later, the fingers in the apex region coalesce, occlude the channel, and stop blood flow, which inhibits the proximal region from growing and occluding the channel (Figure 7-6). The platelet aggregates that were captured near the apex may extend downstream (Figure 2B; R4). Fibrin may have formed at the pores after the SIPA clot occluded the lumen, thus lowering the shear rate and enabling the coagulation cascade to occur (Figure 7-7). The entire process is illustrated in Figure 7. In contrast, the proximal section (Figure 2B; R1) continues to grow but does not bridge the larger lumen size (Figure 7-5). The resulting SIPA clot resembles the SIPA clot from a smaller glass capillary tube[7,34]; however, the specific fingerlike platelet aggregates, extending into the lumen, and the porous structures are new findings in this study.

The pores observed in the transverse clot section imply that the SIPA clot creates a high permeability, as was predicted by Du et al,[35] and would allow for convective drug transport through the inner clot.[36] Although a drug could be transported to the center of the clot through the pores, tPA may not work on a SIPA clot where the histological images show only small amounts of fibrin. Indeed, Kim et al[20] found that DiNAC (diacetyl-L-cystine) lyses the SIPA clot better than tPA. Thus, perfusing a thrombolytic agent that reacts with VWF or platelets may be needed to dissolve a SIPA clot.[20]

The present study had several limitations. First, only one animal's (porcine) blood was used to generate the clot. However, Para and Ku[27] found that there was no significant difference between human and porcine blood when generating a SIPA clot. Second, we used a glass tube that had rigid impermeable walls, and steady flow was applied for generating the SIPA clot. With the alternative triad for SIPA clot formation, we generated a SIPA clot under a controlled in vitro flow system, and the clot was retrievable without any structural damage. This system can be used to generate SIPA clots for testing thrombolytic agents or thrombectomy devices. The SIPA clot structure developed in this study may be used to recreate clots collected through thrombectomy.

Acknowledgments

The authors thank Yolande Berta for help with the sputter coating and SEM imaging of the SIPA clot and Aqua Asberry for help with Carstairs staining. They acknowledge support from National Institutes of Health (NIH 5U54EB027690) and National Science Foundation (NSF - Blood Clotting at the Extreme – Mathematical and Experimental Investigation of Platelet Deposition in Stenotic Arteries 1716357).

Authorship

Contribution: D.A.K. and D.N.K designed the research; D.A.K. performed the research; and both authors wrote the paper.

Conflict-of-interest disclosure: The authors declare no competing financial interests.

ORCID profile: D.A.K., 0000-0003-1181-7342.

Correspondence: David N. Ku, George W. Woodruff School of Mechanical Engineering, Georgia Institute of Technology, 315 Ferst Drive NW, IBB 2307, Atlanta, GA 30332; e-mail: david.ku@me.gatech.edu.

References

1. Bark DL Jr, Ku DN. Wall shear over high degree stenoses pertinent to atherothrombosis. *J Biomech.* 2010;43(15):2970-2977.

2. Stamler J, Neaton JD, Wentworth DN. Blood pressure (systolic and diastolic) and risk of fatal coronary heart disease. *Hypertension.* 1989; 13(5 suppl):I2.

3. Bagot CN, Arya R. Virchow and his triad: a question of attribution. *Br J Haematol*. 2008;143(2):180-190.
4. Cadroy Y, Horbett TA, Hanson SR. Discrimination between platelet-mediated and coagulation-mediated mechanisms in a model of complex thrombus formation in vivo. *J Lab Clin Med*. 1989;113(4):436-448.
5. Weisel JW, Litvinov RI. Visualizing thrombosis to improve thrombus resolution. *Res Pract Thromb Haemost*. 2021;5(1):38-50.
6. Casa LD, Deaton DH, Ku DN. Role of high shear rate in thrombosis. *J Vasc Surg*. 2015;61(4):1068-1080.
7. Ku DN, Flannery CJ. Development of a flow-through system to create occluding thrombus. *Biorheology*. 2007;44(4):273-284.
8. Staessens S, De Meyer SF. Thrombus heterogeneity in ischemic stroke. *Platelets*. 2021;32(3):331-339.
9. Yuriditsky E, Narula N, Jacobowitz GR, et al. Histologic assessment of lower extremity deep vein thrombus from patients undergoing percutaneous mechanical thrombectomy. *J Vasc Surg Venous Lymphat Disord*. 2022;10(1):18-25.
10. Staessens S, Denorme F, Francois O, et al. Structural analysis of ischemic stroke thrombi: histological indications for therapy resistance. *Haematologica*. 2020;105(2):498-507.
11. Schuhmann MK, Gunreben I, Kleinschnitz C, Kraft P. Immunohistochemical analysis of cerebral thrombi retrieved by mechanical thrombectomy from patients with acute ischemic stroke. *Int J Mol Sci*. 2016;17(3):298.
12. Ahn SH, Hong R, Choo IS, et al. Histologic features of acute thrombi retrieved from stroke patients during mechanical reperfusion therapy. *Int J Stroke*. 2016;11(9):1036-1044.
13. Welsh JD, Muthard RW, Stalker TJ, Taliaferro JP, Diamond SL, Brass LF. A systems approach to hemostasis: 4. How hemostatic thrombi limit the loss of plasma-borne molecules from the microvasculature. *Blood*. 2016;127(12):1598-1605.
14. Cines DB, Lebedeva T, Nagaswami C, et al. Clot contraction: compression of erythrocytes into tightly packed polyhedra and redistribution of platelets and fibrin. *Blood*. 2014;123(10):1596-1603.
15. Li Y, Wang H, Zhao L, et al. A case report of thrombolysis resistance: thrombus ultrastructure in an ischemic stroke patient. *BMC Neurol*. 2020;20(1):135-135.
16. Chernysh IN, Nagaswami C, Kosolapova S, et al. The distinctive structure and composition of arterial and venous thrombi and pulmonary emboli. *Sci Rep*. 2020;10(1):5112.
17. Marder VJ, Chute DJ, Starkman S, et al. Analysis of thrombi retrieved from cerebral arteries of patients with acute ischemic stroke. *Stroke*. 2006;37(8):2086-2093.
18. Matsuo O, Rijken DC, Collen D. Thrombolysis by human tissue plasminogen activator and urokinase in rabbits with experimental pulmonary embolus. *Nature*. 1981;291(5816):590-591.
19. Griffin MT, Kim DA, Ku DN. Shear-induced platelet aggregation: 3D-grayscale microfluidics for repeatable and localized occlusive thrombosis. *Biomicrofluidics*. 2019;13(5):054106.
20. Kim DA, Shea SM, Ku DN. Lysis of arterial thrombi by perfusion of N,N′-Diacetyl-L-cystine (DiNAC). *PLoS One*. 2021;16(2):e0247496.
21. Mehrabadi M, Casa LDC, Aidun CK, Ku DN. A predictive model of high shear thrombus growth [published correction appears in *Ann Biomed Eng*. 2019;47(12):2516]. *Ann Biomed Eng*. 2016;44(8):2339-2350.
22. Di Meglio L, Desilles J-P, Ollivier V, et al. Acute ischemic stroke thrombi have an outer shell that impairs fibrinolysis [published correction appears in *Neurology*. 2019;93(18):819.]. *Neurology*. 2019;93(18):e1686-e1698.
23. Carstairs KC. The identification of platelets and platelet antigens in histological sections. *J Pathol Bacteriol*. 1965;90(1):225-231.
24. Obermair A, Wanner C, Bilgi S, et al. Tumor angiogenesis in stage IB cervical cancer: correlation of microvessel density with survival. *Am J Obstet Gynecol*. 1998;178(2):314-319.
25. Posch S, Neundlinger I, Leitner M, et al. Activation induced morphological changes and integrin αIIbβ3 activity of living platelets. *Methods*. 2013;60(2):179-185.
26. Wootton DM, Markou CP, Hanson SR, Ku DN. A mechanistic model of acute platelet accumulation in thrombogenic stenoses. *Ann Biomed Eng*. 2001;29(4):321-329.
27. Para AN, Ku DN. A low-volume, single pass in-vitro system of high shear thrombosis in a stenosis. *Thromb Res*. 2013;131(5):418-424.
28. Tomaiuolo M, Matzko CN, Poventud-Fuentes I, Weisel JW, Brass LF, Stalker TJ. Interrelationships between structure and function during the hemostatic response to injury. *Proc Natl Acad Sci USA*. 2019;116(6):2243-2252.
29. Kim DA, Ashworth KJ, Di Paola J, Ku DN. Platelet α-granules are required for occlusive high-shear-rate thrombosis. *Blood Adv*. 2020;4(14):3258-3267.
30. Tutwiler V, Wang H, Litvinov RI, Weisel JW, Shenoy VB. Interplay of platelet contractility and elasticity of fibrin/erythrocytes in blood clot retraction. *Biophys J*. 2017;112(4):714-723.
31. Casa LDC, Ku DN. Thrombus formation at high shear rates. *Annu Rev Biomed Eng*. 2017;19(1):415-433.
32. Casa LD, Gillespie S, Meeks S, Ku DN. Relative contributions of von Willebrand factor and platelets in high shear thrombosis. *J HematolThromb Dis*. 2016;4(4):1000249.

33. Bark DL Jr, Para AN, Ku DN. Correlation of thrombosis growth rate to pathological wall shear rate during platelet accumulation. *Biotechnol Bioeng.* 2012;109(10):2642-2650.

34. Para A, Bark D, Lin A, Ku D. Rapid platelet accumulation leading to thrombotic occlusion. *Ann Biomed Eng.* 2011;39(7):1961-1971.

35. Du J, Kim DA, Alhawael G, Ku DN, Fogelson AL. Clot permeability, agonist transport, and platelet binding kinetics in arterial thrombosis. *Biophys J.* 2020;119(10):2102-2115.

36. Diamond SL. Engineering design of optimal strategies for blood clot dissolution. *Annu Rev Biomed Eng.* 1999;1(1):427-462.